

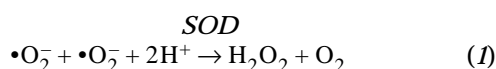
Mouse Extracellular Superoxide Dismutase: Primary Structure, Tissue-specific Gene Expression, Chromosomal Localization, and Lung *In Situ* Hybridization

Rodney J. Folz, Jiazhen Guan, Michael F. Seldin, Tim D. Oury, Jan J. Enghild, and James D. Crapo

Departments of Medicine, Microbiology and Immunology, and Pathology, Duke University Medical Center, Durham, North Carolina

Extracellular superoxide dismutase (EC-SOD) is the major extracellular antioxidant enzyme. We have determined the primary structure of mouse EC-SOD by characterization of complementary DNA (cDNA) clones and by amino-acid sequence analysis of purified protein. cDNA sequence analysis indicates that mouse EC-SOD is synthesized as a 251-amino-acid precursor protein with a predicted molecular weight of 27,400 D. Amino-terminal micro sequence analysis of purified mature mouse lung EC-SOD demonstrated the sequence to begin with SSFDLADRLDPV-. These results indicate that EC-SOD as initially synthesized contains a 24-amino-acid precursor peptide, and that the mature protein is 227 amino acids in length. Computer algorithms that predict the most likely site of cotranslational signal peptidase cleavage suggest that processing will occur between amino acids 18 and 19 or 20 and 21, which implies that EC-SOD may be initially synthesized as a pre-pro-protein. Like human EC-SOD, mature mouse EC-SOD is glycosylated. The full-length mouse EC-SOD cDNA is 1,834 base pairs long and is 82% (79% for protein) identical to rat EC-SOD, but only 60% (60% for protein) identical to human EC-SOD. The mouse EC-SOD gene locus (*Sod3*) was mapped by interspecific backcross haplotype analysis as being 0.9 ± 0.9 centimorgans distal to the *Qdpr* locus on mouse Chromosome 5, a position suggesting that the human homologue of EC-SOD will map close to the human QDPR locus (4p15.3). Of nine tissues examined by Northern blot analysis, those of the kidney and lung are by far the major tissues that express EC-SOD messenger RNA. Using *in situ* hybridization in the mouse lung, we demonstrate EC-SOD gene expression to be highly localized to alveolar Type II epithelial cells. These data suggest that alveolar Type II cells play a central role in mediating EC-SOD antioxidant function in the lung. **Folz, R. J., J. Guan, M. F. Seldin, T. D. Oury, J. J. Enghild, and J. D. Crapo. 1997. Mouse extracellular superoxide dismutase: primary structure, tissue-specific gene expression, chromosomal localization, and lung *in situ* hybridization. *Am. J. Respir. Cell Mol. Biol.* 17:393-403.**

The enzymatic disproportionation or dismutation (Equation 1) of superoxide free-radical anion species by



(Received in original form October 31, 1996 and in revised form February 10, 1997)

Address correspondence to: Rodney J. Folz, M.D., Ph.D., Duke University Medical Center, Box 3177, Durham, NC 27710. E-mail: rjf@galactose.mc.duke.edu.

The nucleotide sequences reported in this paper have been submitted to the GenBank Data Base with accession number U38261.

Abbreviations: 5-bromo-4-chloro-3-indoxyl phosphate/nitro blue tetrazolium, BCIP/NBT; copper, zinc SOD, CuZn-SOD (SOD1); extracellular SOD, EC-SOD (SOD3); manganese SOD, Mn-SOD (SOD2); reverse transcriptase polymerase chain reaction, RT-PCR; superoxide dismutase, SOD.

Am. J. Respir. Cell Mol. Biol. Vol. 17, pp. 393-403, 1997

superoxide dismutase (SOD) was characterized by McCord and Fridovich more than 25 yr ago (1). Since that discovery, a total of three genetically distinct mammalian isoforms of SOD have now been reported. SOD1, a copper- and zinc-containing SOD (CuZn-SOD), is localized primarily to cytoplasmic and nuclear compartments (2-4). Its mapping to chromosome 21 (5) was important for the subsequent successful genetic linkage of mutations in SOD1 to hereditary forms of familial amyotrophic lateral sclerosis (6, 7). SOD2, a manganese-containing SOD (Mn-SOD) is linked to human Chromosome 6 (8) and is found predominantly in mitochondria (9, 10). SOD2 has been shown to play a major role in promoting cellular differentiation (11), protecting against hyperoxic-induced pulmonary toxicity (12), and providing cellular resistance to cytotoxicity by tumor necrosis factor (TNF) (13, 14). By contrast, SOD3, or extracellular superoxide dismutase (EC-SOD), is the predominant extracellular antioxidant enzyme. EC-SOD has

been found in serum and in cerebrospinal, ascitic, and synovial fluids (15, 16). In some human tissues such as uterus, umbilical cord, placenta, and arteries, EC-SOD enzyme activity equals or exceeds that of CuZn-SOD and Mn-SOD (17, 18). An EC-SOD-like activity has been identified in every mammal examined thus far (19).

Human EC-SOD is a secretory, homotetrameric glycoprotein with a molecular weight of about 135,000 D (15, 20–22). Affinity of EC-SOD for heparan sulfate proteoglycans located on cell surfaces and in the extracellular matrix is mediated by a cluster of positively charged amino acid residues located on the protein's COOH terminus (23). Partial proteolytic removal of the COOH-terminal heparin-binding region occurs both *in vitro* and *in vivo*, and results in a heterogeneous population of EC-SOD tetramers with varying affinity for heparin-Sepharose (17, 22, 24–26). The Type A tetramer has all four subunits cleaved and demonstrates no affinity for heparin-Sepharose. Type B has partial cleavage and demonstrates intermediate binding. Type C has all four subunits intact and shows the highest affinity. Characterization of the human (27) and rat EC-SOD cDNAs (28–30) has shown DNA and amino-acid sequence homology to CuZn-SOD but not Mn-SOD. The human EC-SOD gene is distinct (31), and has been regionally localized to Chromosome 4 (32). Human EC-SOD is expressed by a variety of fibroblasts and glial cell lines grown in culture (33, 34). Cytokines dramatically modulate EC-SOD gene expression (35), but various forms of direct oxidant stresses do not (36).

EC-SOD in the mouse lung is unique in that it is present at 10 times the levels seen in any of nine other mammalian species examined to date (19). This EC-SOD has been shown to impart protection to oxidative stress in the lung, based on the finding that mice that lack EC-SOD activity are more sensitive to lethal levels of hyperoxia (37). Although hyperoxia results in enhanced intracellular oxidant stress (38), it is unclear by what mechanism(s) an extracellular antioxidant such as EC-SOD participates in this process. Characterization of the mouse EC-SOD gene should allow additional insights into the role of EC-SOD under normal and pathologic conditions in the lung. In the study described here, we cloned the complete mouse EC-SOD cDNA and determined its primary structure by amino-acid sequence analysis of highly purified mature protein product. Computer algorithms that predict the site of signal peptide cleavage suggest that the mouse EC-SOD protein may be initially synthesized as a pre-pro-protein. *Sod3* was mapped to a position 0.9 ± 0.9 centimorgans distal to the *Qdpr* locus on mouse Chromosome 5. In the mouse lung, *in situ* hybridization data show EC-SOD to be highly expressed by alveolar Type II epithelial cells, which are critical in maintaining lung function.

Materials and Methods

Materials and Radiochemicals

[α -³⁵S]dATP (~ 1,400 Ci/mmol), [γ -³²P]ATP (3,000 Ci/mmol), and [α -³²P]CTP (800 Ci/mmol) were purchased from New England Nuclear (Boston, MA). Sequenase sequencing kit (V 2.0) was from United States Biochemicals Corporation (Cleveland, OH). SeaPlaque GTG agarose

was from FMC BioProducts (Rockland, ME). Restriction enzymes were from New England Biolabs (Beverly, MA). All other reagents used were of molecular-biology grade. Oligonucleotides were synthesized by Oligos, Etc. (Wilsonville, OR), and were used without further purification. Charged nylon membranes (GeneScreen Plus) were from DuPont, Wilmington, DE.

Total RNA Isolation, Reverse Transcriptase-Polymerase Chain Reaction, and Multiple-Tissue Northern Blot Analysis

Total RNA was purified from various mouse tissues, using the guanidium HCl method (39). Initially, a partial mouse EC-SOD cDNA was cloned with the reverse transcriptase-polymerase chain reaction (RT-PCR). Primers were designed to be complementary to the recently cloned rat EC-SOD cDNA (28, 29), and consisted of MF-1 (5'-GAA-CCTCAGCCATGGTGGCC-3'), which corresponds to nucleotide positions 98 to 117, and MR-1 (5'-GCTTAA-GTGGTCTTGCACTCG-3'), which corresponds to nucleotide positions 845 to 825. Total lung RNA (0.5 μ g) was reverse transcribed in a final volume of 20 μ l containing mouse reverse primer MR-1 (10 ng/ μ l), 1X RT buffer, and 0.5 units of moloney mouse leukemia virus (MMLV) RT, and incubated for 60 min at 37°C. Five microliters of the RT mixture was PCR amplified, using MF-1 (10 ng/ μ l), MR-1 (10 ng/ml), 1.5 mM MgCl₂, 20 mM diethyl-p-nitrophenyl monothiophosphate (dNTP), and 0.5 units of TAQ polymerase. Cycling conditions consisted of a 95°C melt for 40 s, followed by annealing at 52°C for 30 s and extension at 72°C for 45 s. Thirty-five cycles of three-step PCR were followed by a 5-min extension reaction at 72°C. PCR products were analyzed with agarose gel electrophoresis and stained with ethidium bromide. The unique 750-bp PCR product was subcloned into the pCR II bacterial plasmid, using the TA Cloning Kit (Invitrogen, San Diego, CA) as recommended by the manufacturer. DNA sequencing of the 5' and 3' region confirmed the authenticity of this clone (ME/TA clone No. 3).

Fifteen micrograms of total RNA from various tissues were electrophoresed on a denaturing formaldehyde agarose gel, transferred to charged nylon membranes, and hybridized with ³²P-labeled sense and antisense mouse EC-SOD riboprobes as previously described (31).

Isolation and DNA Sequencing of a Full-length EC-SOD cDNA from Mouse Lung

A male/female combined B₆CBA mouse lung cDNA library constructed in the Uni-Zap XR vector was purchased from Stratagene (La Jolla, CA) and probed with the partial mouse EC-SOD cDNA described earlier. Approximately 25,000 pfu were plated onto a lawn of XLI-Blue and grown overnight at 37°C. Plaques were duplicate-lifted onto charged nylon membranes (GeneScreen Plus; DuPont), incubated in 0.5 M NaOH for 2 min ($\times 2$) and in 1 M Tris, pH 7.5, for 2 min ($\times 2$), and baked in a vacuum oven at 80°C for 2 h. The membranes were wetted in 2X standard saline citrate (SSC) buffer for 20 min at room temperature and subsequently prehybridized in 50% for-

mamide, 0.25 M sodium phosphate (pH 7.2), 0.25 M NaCl, 1 mM ethylenediamine tetraacetic acid (EDTA), 7% sodium dodecylsulfate (SDS), and 5% polyethylene glycol (molecular weight: 8,000) for 1 h at 60°C. The blot was hybridized overnight in the same buffer containing 0.85×10^6 cpm/ml of ^{32}P -labeled ME/TA clone No. 3 RNA, generated by *in vitro* transcription of Xho I linearized, partial-length mouse EC-SOD cDNA with SP6 RNA polymerase in the presence of [α - ^{32}P]CTP. After hybridization, the blots were washed in 2X SSC for 20 min at room temperature. This was followed by a second 30-min wash at 70°C, using 0.25 M sodium phosphate (pH 7.2), 2% SDS, and 1 mM EDTA, and by a third 30-min wash at 70°C using 0.4 M sodium phosphate (pH 7.2), 1% SDS, and 1 mM EDTA. Three positive clones were initially identified and further purified. Mouse clone 5A-27 was found to contain the largest DNA insert, and was used as a template for DNA sequencing.

The dideoxy sequencing method was employed, using double-stranded DNA as a template and Sequenase enzyme (United States Biochemicals), and both strands were completely sequenced with a double-stranded DNA sequencing protocol as previously described (40). The reverse and T7 promoter primer were used to initiate DNA sequence data. Oligonucleotides derived from these initial sequencing data were synthesized approximately every 250 bp until the complete nucleotide sequence was obtained from both strands of DNA.

Amino Acid Sequencing of Purified Mature and Tryptic Peptides of Mouse Lung EC-SOD

EC-SOD was purified from mouse lungs essentially as described for human EC-SOD, except that mono Q chromatography preceded the mono S chromatography step (41). Briefly, mouse lungs were homogenized and EC-SOD initially purified by heparin-Sepharose affinity chromatography. Fractions containing SOD activity were collected and subjected to mono Q Sepharose followed by mono S Sepharose chromatography. EC-SOD specific activity was measured by inhibition of cytochrome c reduction at pH 10.0 as previously described (42). Total protein was measured by absorption at 280 nm.

Purified EC-SOD (60 μg) was subjected to SDS-PAGE in the presence of 10 mM dithiothreitol (DTT) and then transferred to Immobilon-P transfer membranes (Millipore, Bedford, MA) for NH_2 -terminal sequence analysis (43). Internal sequence analysis was obtained by digestion of 80 μg of mouse EC-SOD with 1 μg endoproteinase Asp-N (Sigma Chemical Co., St. Louis, MO) at room temperature overnight. Peptides from this digest were separated by reverse-phase high-performance liquid chromatography (HPLC) on a 2.1 mm \times 220 mm Aquapore RP-300 column (Brownlee, Branchburg, NJ) as previously described (44).

The purified peptides were analyzed by automated Edman degradation, using an Applied Biosystems Model 477A sequencer (Foster City, CA) with on-line phenylthiohydantoin analysis done with an Applied Biosystems Model 120A HPLC. Samples were applied to Porton (Beckman Instruments, Inc., Fullerton, CA) peptide or protein

sample support discs, and were sequenced with the modified cycles PI-BGN and PI-1 recommended by Porton Instruments.

Computer-assisted Sequence Analysis

The IntelliGenetics Geneworks (Campbell, CA) program (Version 2.4) was used for organizing the DNA sequence data as well as for DNA and amino acid alignment. Homology searching was performed at the National Center for Biotechnology Information (NCBI), using the Basic Local Alignment Search Tool (BLAST) (45) network service and the nonredundant nucleotide sequence database (GenBank + EMBL + DDBJ + PDB; release date: April 8, 1996), and the nonredundant peptide sequence database (GenBank CDS translations + PDB + SwissProt + SPupdate + PIR, release date: April 8, 1996). For prediction of the signal-peptide cleavage site, the programs SIGSEQ1 (46) and SIGSEQ2 were employed (47). Phylogenetic relationships were calculated with an unweighted pair group method with arithmetic means (48).

Mouse Lung *In Situ* Hybridization

$\text{B}_6\text{C}_3\text{F}_1$ mice (Taconic, NY) were anesthetized with pentobarbital (about 80 mg/kg) by intraperitoneal injection. The trachea was cannulated and the diaphragm was punctured to deflate the lung. The lung was subsequently inflation fixed with 4% paraformaldehyde buffered in 0.1 M sodium phosphate buffer, pH 7.4, at a water pressure of 20 cm, at 25°C for 60 min. Next, the lung was excised *en bloc* and placed in 2% paraformaldehyde and 0.1 M sodium phosphate, pH 7.4, for overnight fixation at 4°C. Following fixation, the lungs were mounted in paraffin, and 4- μm -thick tissue sections were floated onto a protein free bath of distilled water and placed onto 3-aminopropyltriethoxysilane (APTS)-coated slides. The sections were deparaffinized by immersion in two changes of xylene for 10 min each. The xylene was removed with two changes of 100% ethyl alcohol for 5 min each, and the sections were then air dried. The tissue sections were next detergent-permeabilized by immersion into phosphate-buffered saline (PBS) for 2 min, followed by 15 min in 0.3% Triton X-100 in PBS at room temperature. The sections were next washed in two changes of PBS. The sections were proteolyzed by first placing them in 10 mM Tris-HCl, and 50 mM EDTA, pH 8.0, for 5 min, followed by incubation in 0.1 mg/ml proteinase K in 100 mM Tris-HCl and 50 mM EDTA, pH 8.0, for 4 min at room temperature. The slides were then immersed in 0.1 M glycine in PBS for 5 min at room temperature and rinsed in PBS for 1 min. The sections were acetylated by immersion in freshly prepared triethanolamine (0.1 M, pH 8.0) for 3 min, followed by immersion in triethanolamine (0.1 M, pH 8.0) containing 0.25% acetic anhydride for 1 min at room temperature. Following this, the slides were washed generously, using distilled water, and were air dried at 37°C for 10 min prior to storage at -70°C.

In vitro transcription of digoxigenin-labeled sense and antisense-strand mouse EC-SOD cRNA was accomplished with digoxigenin-11-UTP, following a standard labeling-reaction assay recommended by the manufacturer

(Boehringer Mannheim, Indianapolis, IN). Approximately 100 to 200 ng of digoxigenin-labeled probe was diluted in 50 μ l of hybridization buffer (22.5% formamide, 5X SSPE, 2% SDS, 10 mg/ml polyvinylpyrrolidone, and 0.97 mg/ml salmon sperm DNA [Sigma]), heat denatured by incubating for 5 min at 95°C, and hybridized overnight at 37°C in a moist chamber. On the following day the slides were washed in 2X SSC buffer, followed by four consecutive washes in 2X SSC containing 0.1% SDS for 5 min each at 55°C.

The digoxigenin label was developed with an antidigoxigenin antibody conjugated to alkaline phosphatase (Boehringer Mannheim). The slides were first washed in Buffer I, containing 100 mM Tris-HCl, pH 7.5, and 150 mM NaCl. Serially sectioned negative controls were incubated in Buffer I containing 2% normal sheep serum and 0.3% Triton X-100. Positive control sections were incubated in Buffer I containing antidigoxigenin antibody diluted 1:100 and containing 1% sheep serum and 0.3% Triton X-100, and were then incubated for 1 h at 37°C. The slides were washed with several changes of Buffer I, followed by washing with several changes of Buffer II (100 mM Tris-HCl, pH 9.5; 150 mM NaCl; 50 mM MgCl₂). The antibody conjugate was developed by covering the specimens with a solution of 5-bromo-4-chloro-3-indoxyl phosphate and nitro blue tetrazolium chloride (BCIP/NBT), and incubating the specimens in the dark under conditions recommended by the manufacturer (DAKO Corporation, Carpinteria, CA). The sections were next counterstained with nuclear Fast Red.

Mouse Chromosomal Mapping

C3h/HeJ-*gld* and *Mus spretus* (Spain) mice and [(C3h/HeJ-*gld* \times *Mus spretus*)F₁ \times C3h/HeJ-*gld*] interspecific backcross mice were bred and maintained as previously described (49). *Mus spretus* was chosen as the second parent in this cross because of the relative ease of detection of informative restriction-fragment-length variants (RFLV) in comparison with crosses made with conventional inbred laboratory strains.

DNA isolated from mouse organs by standard techniques was digested with restriction endonucleases, and 10- μ g samples were electrophoresed in 0.9% agarose gels. DNA was transferred to Nytran membranes (Schleicher and Schull, Inc., Keene, NH), hybridized at 65°C, and washed under stringent conditions, all as previously described (50). Clones used as probes for the linkage analyses included a rat cDNA obtained by RT-PCR cloning of the complete coding region of EC-SOD done with total RNA isolated from rat lung. Rat-specific forward, rEC-F23 (5'-TTCTCAGGCCTCTAGCTGG-3'), and reverse, rEC-R1104 (5'-TGGTCTCCGAGAACAGTGC-3'), oligonucleotides and were derived from previously published rat cDNA sequences (28, 29). Additional clones for detecting dihydropteridine reductase (*Qdpr*) and the tod photoreceptor cGMP-gated cation channel were as previously described (51).

Gene linkage was determined by segregation analysis (52). Gene order was determined by analyzing all haplotypes and minimizing crossover frequency between all genes that were determined to be within a linkage group.

This method resulted in determination of the most likely gene order (53).

Results

Characterization of Mouse EC-SOD cDNA Clones

The initial isolation of a partial-length murine EC-SOD cDNA clone was accomplished with RT-PCR, using primers designed from areas of DNA sequence homology between a recently cloned rat (28, 29) and human EC-SOD cDNA (27). A single PCR product of 759 bp was amplified and subcloned into a TA cloning vector. DNA sequence analysis of the 5' and 3' ends confirmed the authenticity of the cloned partial-length cDNA (data not shown). This partial-length clone was then used as a radiolabeled probe to screen a mouse lung cDNA library, from which three positive hybridizing clones were identified. The clone containing the largest insert, clone No. 5A-27, was completely sequenced on both strands (Figure 1). The insert cDNA was 1,834 bp in length, and contained a 269-bp 5'-non-translated region, a 756-bp putative protein coding region, and a 790-bp 3' noncoding region, followed by a 19-bp poly A tract. A putative polyadenylation signal was found to occur 20 bp upstream of the poly A tract (Figure 1).

A 251-amino-acid protein sequence was deduced from the cDNA. This sequence contains a predicted signal peptide followed by a mature protein domain. Computer algorithms that predict the site of signal-peptide cleavage either through the "-3, -1" rule, SIGSEQ1 (47), or on the basis of a weighted matrix, SIGSEQ2 (47), indicate several potential satisfactory sites for cotranslation cleavage (Figure 1). None of these algorithms supports signal-peptide cleavage between residues 24 and 25, and the algorithms furthermore suggest cleavage at this position to be highly unlikely.

Mouse EC-SOD is glycosylated, based on: (1) its binding affinity for concanavalin A (ConA) during protein purification; (2) the decreased apparent mobility of the purified protein on SDS-PAGE (34 kD, as compared with the predicted 24.9 kD); (3) its increased mobility with endoglycosidase treatment (data not shown); and (4) decreased mobility of the *in vitro*-translated cRNA product in a cotranslational reticulocyte lysate and canine pancreatic microsomal membrane assay (54) (data not shown). Mouse EC-SOD is predicted to be glycosylated (most likely at Asp⁹⁷), based on sequence homology with human EC-SOD (21). The high-mannose precursor glycosylation consensus amino acid sequence A-X-N (55) is conserved at this position (positions 97 to 99). The carboxy-terminal region contains a charged, uninterrupted, six-amino-acid basic domain, which most likely represents the site previously identified in human EC-SOD as having affinity for heparin Sepharose (17, 23, 56).

Purification and Amino-acid Sequence Analysis of Mature EC-SOD

Mouse EC-SOD was purified to a final specific activity of 15,000 units/A₂₈₀. Purified EC-SOD was found to migrate as two bands (34 kD and 32 kD) on reducing SDS-PAGE, as has previously been seen with human EC-SOD (Figure 2) (57). A faint 30-kD band was also observed. All three

1	CCGGGGGAAG AGGAGGAGGC AGCAATTTTA CCACAAGGGA CAGCCAAGCT GGCTTTGCTT CTCTTGCCCA GCCCAATGAC CTTCCTCCCA TTTGCTGACC	100
101	ACTCCCCCGG GCTGGCCTCC CTGTGCTCG CTCACATAAC AGCCAGCTGG ACAGCTCTGG GGAGGCAACT CAGAGGCTCT TCCTCCGGCC TCTAGCTGGG	200
201	TGCTGGCCTG AACTTCACCA GAGGAAAGA GCTCTTGGGA GAGCCTGACA GGTGCAGAGA ACCTCAGCCA TGTTGGCCCT CTGTGCTTAC GGCTTGCTAC	300
-24		-15
301	TGGCGGCTG TGGCTCTGTC ACCATGTCAA ATCCAGGGGA GTCCAGCTTC GACCTAGCAG ACAGGCTTGA CCCGGTTGAG AAGATAGACA GGCTTGACCT	400
-14	<u>L A A C G S V T M S N E G E S S F D L A D R L D E V E K I D R L D L</u>	20
401	GGTTGAGAAG ATAGGCGACA CGCATGCCAA AGTGTGGAG ATCTGGATGG AGCTAGGACG ACGAAGGGAG GTGGATGCTG CCGAGATGCA TGCAATCTGC	500
21	<u>V E K I G D T H A K V L E I W M E L G R R R E V D A A E M H A I C</u>	53
501	AGGGTACAAC CATCAGCCAC GCTGCCACCG GATCAGCCG AGATCACC GGCTTGTCTC TTCGGGACG TGGGGCCGGG CTCCAGGCTT GAGGCCTATT	600
54	<u>R V Q P S A T L P P D Q E Q I T G L V L P R O L G P G S R L E A Y</u>	86
601	TCAGTCTGGA GGGCTTCCCA GCTGAGCAGA ACGCCTCCAA CCGTGCCATC CACGTGCATG AGTTCCGGGA CCTGAGCCAG GGCTGCGATT CCACCGGGCC	700
87	<u>F S L E G F P A E Q N A S N R A I H V H E F G D L S Q G C D S T G P</u>	120
701	GCACTACAAC CCGATGGAGG TGCCGCACCC TCAGCACCCG GCGACTTTG GCAACTTCGT GGTGCGCAAC GGCCAGCTCT GGAGGCATCG CGTCGGCTG	800
121	<u>H Y N P M E V P H P Q H P G D F G N E V V R N G O L W R H R V G L</u>	153
801	ACCGCTGCG TGGCCGGACC GCACGCCATC TTGGCCGCT CTGTGGTGGT CCACGCCGC GAGGACGACC TGGGTAAAGG TGGCAACCAG GGCAGCCTGC	900
154	<u>T A S L A G P H A I L G R S V V V H A G E D D L G K G G N O A S L</u>	186
901	AGAACGGCAA TGCAGGTCGC CGGCTCGCCT GCTGCGTGGT AGGCACCAGC AGCTCCGCGC CCTGGGAGAG CCAGACAAAG GAGCGCAAGA AGCGGCGGGC	1000
187	<u>Q N G N A G R R L A C C V V G T S S S A A W E S Q T K E R K K R R R</u>	220
1001	GGAGAGCGAG TGCAAGACCA CTTAAGCCTC ACTCAGGGCC TCCGAGCCCC GCGCTGCAC GCATAGATGT CTCCAGGCGC CCCAGACGC CTCTAGTCAC	1100
221	<u>E S E C K T T *</u>	227
1101	CCCAGAGGCC TCTAGGCGTC CTAGACAGAG GCCTCCAGA CACCTCAGTC GCCTCTGCGC TTCCATGCAC GCCAGACACC TCTGTATGGC CCCCAGATGC	1200
1201	CTCCACGAAC CTCCGCGCAC CCTAGATGTT CTCCCATGTC CCGGACACGG TTCTCTGTG TCCAGGACAC CTTAGTTAAC CCAGAAATCT TTTACGCCCC	1300
1301	TATGCACTTC CACAGACCCA GATCCTTAAT GCTCTAGATC CATCCCGAGC CCCTTTGTGT CCCAAGACAA TCCACAAGC CCCTAGTCTT TGAGTCTGCT	1400
1401	CTCAGAGAAC CCCCTCTTCC TCCCCAGAGA TCGCATGTGC TCAGATACTC TCCTCCTCTG AGGACTTCCC AGTGAGCACC TTTGAGGTAC TCCCTTGGGG	1500
1501	TATACTGAAA TATCGCCAC CCCATTTCCT TCTGCCCCCT TTTGTTTTCT TCCTGTCCCC ATAGCACCCG AGACTCCTCT CTTCCCTAGA GACCTCTTTT	1600
1601	TTCTTCCCTT TGTTCCTCG AGGGCTCTG GGACCACTCT GACACCCTCA CCCCCACCC CAAGTTCCAT GTTCCCGATC ACCTCCTGCG GAGGCCCCAG	1700
1701	GTCTGTGTTT CATCTGTTT CCATATGGTG CCTGCACCCC AGGGAGAGCA GCTCCTAGA GAGAGTATT GGGAACTTT ATGTTGCTCA TTAATAACAT	1800
1801	AGCAATTCAC AACACAAAA AAAAAAAAAA AAAA	1834

Figure 1. cDNA sequence and amino-acid sequence for mouse EC-SOD. An 1,834-bp cDNA was isolated from a mouse lung cDNA library and DNA was sequenced in both orientations. The deduced amino-acid sequence for the predicted primary translation product is shown in the single-letter amino acid code. Underlined amino-acid sequences were confirmed by direct amino-acid sequence analysis of highly purified mouse lung EC-SOD and of its HPLC-purified tryptic peptides. The beginning of the mature protein sequence is indicated. Likely sites of signal-peptide cleavage predicted by SIGSEQ1 (\downarrow) and SIGSEQ2 (\uparrow) are indicated (47). A putative site of glycosylation based on amino-acid sequence homology with glycosylated human EC-SOD is shown by a *female sign*. The positively-charged hexapeptide region important in heparin binding is marked with a *solid cross*. An *asterisk* indicates the termination codon. A putative polyadenylation recognition site is enclosed by a *dotted box*.

bands contained identical NH_2 -terminal sequences (Table 1) as determined by Edman degradation, indicating that the mass difference in these species is probably a result of C-terminal truncation, as has previously been described for human EC-SOD (23). Sequence analysis of peptides generated by proteolysis of EC-SOD (Table 1) shows that they match the protein sequence predicted from the cDNA sequence, confirming the identity of the cDNA clone. Based on amino-terminal sequence results for purified mature EC-SOD, the mature mouse EC-SOD is predicted to be 227 amino acids in length, with a predicted molecular weight of 24,876 D.

A multiple-amino acid sequence alignment for mouse, rat, and human pre-EC-SOD is shown in Figure 3. The mouse protein contains 79% sequence similarity to the rat protein, but only 60% similarity to human EC-SOD. A seven-amino-acid insertion starting at position 27 is unique

to the mouse sequence (Figure 3). The human sequence, compared with those of the mouse and rat, contains two small deleted areas of six and three amino acids starting at consensus positions 42 and 238, respectively (Figure 3). The most highly conserved region among these three species is the presumptive catalytic-site domain (consensus positions 126 through 225) (58). Unlike human or mouse EC-SOD, rat EC-SOD exists as a dimer and has reduced affinity for heparin-Sepharose. A valine \rightarrow aspartic acid substitution at consensus position 55 has been shown to be responsible for this biochemical difference (30).

Murine EC-SOD Is Highly Expressed in Kidney and Lung

To investigate the expression of mouse EC-SOD in multiple tissues, total RNA from nine different tissues was analyzed with gel blot hybridization of RNA to a radiolabeled

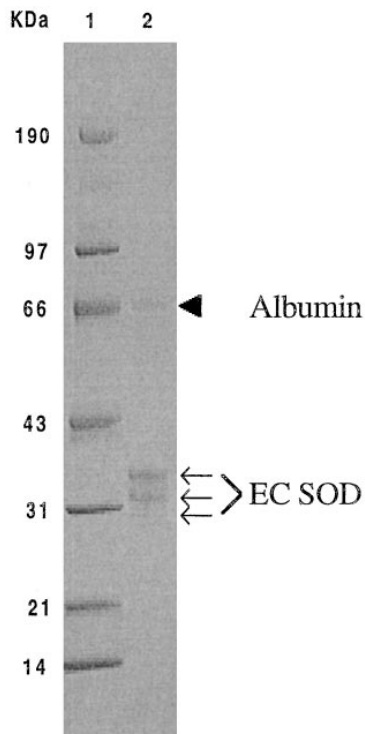


Figure 2. Purification of mature mouse lung EC-SOD and its micro sequence analysis. Protein molecular weight markers (Lane 1) and 5 µg of purified mouse EC-SOD (Lane 2) were subjected to SDS-PAGE, and the gel was stained with Coomassie blue. The arrows indicate bands corresponding to EC-SOD as determined by NH₂-terminal sequence analysis. The upper, middle, and lower (faintly visible) EC-SOD bands contained the same NH₂-terminal sequence. The arrowhead depicts the major contaminant protein (less than 5%), which was determined with N-terminal sequence analysis to be albumin.

TABLE 1
Amino terminal sequence analysis of mouse EC-SOD protein/peptides

Band from gel	Edman degradation analysis
Top band of gel	Mouse albumin sequence
Top band of EC-SOD	SSFDLADRLDPVEKIDRLDLVEKI
Middle band EC-SOD	SSFDLADRLDPVEKIDRLDL
Lower band EC-SOD	SSFDLADRLDPVEKID
Asp-N digest peptide	
18	EIWME
42	DQPQITGLVLFRLQGPGRSL
36	EAYFSLEGFPAEQNA
40	GDFGNFVVRNGQL
38	DFGNFVVRNGQL
35	DDLKGGGNQASLQ

antisense cRNA derived from our PCR-cloned, partial-length EC-SOD cDNA. A discrete band of approximately 1.8 kb in length can be seen in most of the tissues examined (Figure 4). To control for RNA loading and efficiency of blotting, the membrane was additionally probed with a radiolabeled 18S ribosomal RNA (rRNA) oligonucleotide (data not shown). The amount of EC-SOD RNA was quantified with Phosphorimager (Molecular Dynamics, San Francisco, CA) densitometry analysis and normalized to 18S rRNA. The kidney and lung were the dominant organs expressing EC-SOD, and when normalized to the brain, contained 60.5 and 30.2 times the quantity of EC-SOD seen in the brain. The spleen, heart, liver, large intestine, and brain contained 4.9, 3.3, 2.3, 1.2, and 1.0 relative amounts of EC-SOD RNA, respectively. Although not evident in the autoradiograph shown in Figure 4, a unique band of EC-SOD expression was detectable in the brain and large intestine at longer exposures (data not shown).

Consensus	MLAFLF**LL LAACGSVTWT **D**E----	---**VD*AD RLDLVEKIGD THAKVLEIWM ELG*RRRE*DA	70
mouse preECsODYG..MS NPGESSFDLA DRLDP.EKI.R...V.. 70
rat preECsOD	.V....CN..	.V..... MS.TG.----	---SG...L.. ..S.D..... .KQ...A.. 63
human preECsOD	...L.CSC..	...GA.DA.. GE.SA.----	---PNS.S.E W----- .R. MY...T...Q .VMQ...DD.G 57
Consensus	*EMHA*CRVQ PSATLPPDQP QITGLVLFRLQ LGP*SRLEA* F*LEGFPAEQ N*SNRAIHVH EFGDLSQGCE	140	
mouse preECsOD	A...I....G....Y .S.....	.A.....D 140
rat preECsOD	R...V....	..M.....	...S.....S .N..... .T..H..... 133
human preECsOD	-TL..A.Q..DAA.. RV..V....	.A.RAK.D.F .A.....T.P .S.S..... Q..... 126
Consensus	STGPHYNPL* VPHQHPGDF GNFVVRDG*L WRHR*GLAAS LAGPHSILGR AVVHAGEDD LGKGGNQASV	210	
mouse preECsODMEN.Q.	...V..T.. ..A.... S.....L 210
rat preECsODGR.	.K..M...T. 203
human preECsODAS.	..Y.A..... .V... ..R..... 196
Consensus	QNGNAGRRLA CCVVGTS*S* AWESQTK---	ERKKRRRESE CKTT	254
mouse preECsODS.A 251
rat preECsODN.E 244
human preECsOD	E.....VCGPG	L..R.AREHSAA 240

Figure 3. Amino-acid sequence comparison of EC-SOD. The deduced amino-acid sequences of the mouse, rat, and human EC-SOD are shown. Positions of sequence identity are marked by a black dot. Amino-acid insertions are indicated by a hyphen. A consensus sequence for EC-SOD is shown at the top of each alignment. An asterisk indicates consensus could not be reached at this position. The amino acid valine is required for tetramerization and is indicated with an open star. The basic heparin binding region is depicted within a large dashed box.

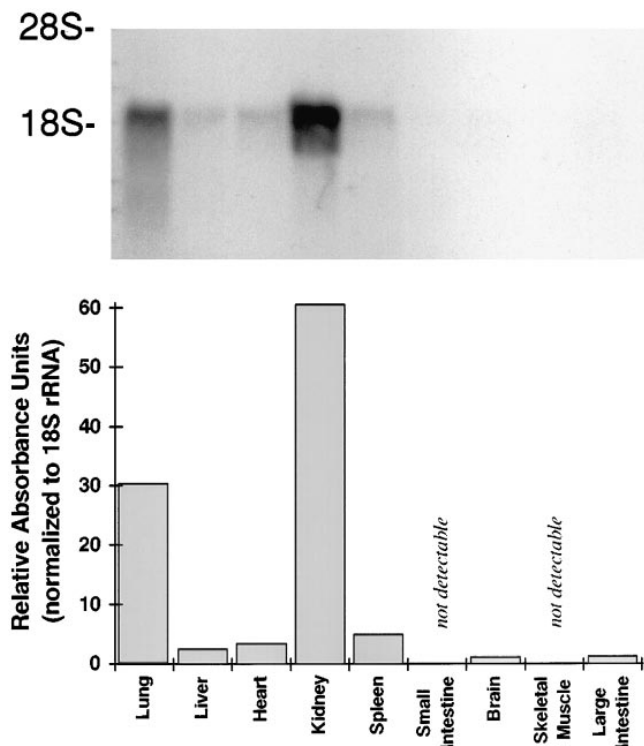


Figure 4. Multiple-tissue RNA blot analyses of EC-SOD in mouse. Approximately 30 μ g total RNA was loaded per lane and hybridized to radiolabeled antisense-strand mouse EC-SOD cRNA. The density of each band was quantitated with Phosphorimager densitometry analysis. To demonstrate a weak signal in some tissues, the autoradiograph shown needed to be intentionally overexposed. Shorter exposure times were used to quantify the density of each signal. The histogram plots the EC-SOD mRNA density after normalizing to 18S rRNA. Lane 1, lung; Lane 2, liver; Lane 3, heart; Lane 4, kidney; Lane 5, spleen; Lane 6, small intestine; Lane 7, brain; Lane 8, skeletal muscle; Lane 9, large intestine. Migration of 18S and 28S rRNA is shown.

However, despite overexposing the blot to film, we were unable to detect EC-SOD RNA expression in small intestine and skeletal muscle. The patterns of EC-SOD expression described here have been reproduced by probing a second, independently obtained, multiple-tissue RNA blot (data not shown). The bands seen are felt to be specific, since hybridization with radiolabeled sense-strand EC-SOD cRNA showed no detectable hybridization signal (data not shown).

Mouse Chromosomal Localization and Fine Mapping

In order to determine the chromosomal location of the *Sod3* gene, we analyzed a panel of DNA samples from an interspecific cross that has been characterized for more than 750 genetic markers throughout the genome. The genetic markers included in this map span 50 to 80 centimorgans on each mouse autosome and the X chromosome (for example, see the reports by Saunders and Seldin [59] and Watson and colleagues [60]). Initially, DNA from the two parental mice [C3H/HeJ-*gld* and (C3H/HeJ-*gld* \times *Mus*

<i>Qdpr</i>	■	□	■	□	■	□
<i>Sod3</i>	■	□	□	■	■	□
<i>Cncg</i>	■	□	□	■	□	■
# of mice	43	62	0	1	3	5

Figure 5. Regional chromosomal localization of mouse EC-SOD. Haplotype data for interspecific backcross mice typed with markers segregating on mouse Chromosome 5. Backcross loci are arranged on the left. The genotypes of individual backcross mice determined in this study are represented by the filled (C3H/HeJ-*gld*) and open [(C3H/HeJ-*gld* \times *Mus spretus*)F₁ heterozygous] boxes. The total number of mice with each haplotype is indicated at the bottom of each column. The mouse *Sod3* RFLVs cosegregate with the *Qdpr* locus (0.9 cM \pm 0.9 cM). By analogy, this suggests location of the human EC-SOD locus at 4p15.3.

spretus)F₁] was digested with various restriction endonucleases and hybridized with rat EC-SOD cDNA probe to determine RFLVs in order to allow haplotype analyses. Informative RFLVs were detected with *Bam* HI-restricted DNAs (C3H/HeJ-*gld*, 4.0 kb; *Mus spretus*, 9.6 kb).

Comparison of the haplotype distribution of the *Sod3* RFLVs indicated that in 113 of the 114 meiotic events examined, the *Mif* locus cosegregated with *Qdpr* (Figure 5), a locus previously mapped to mouse Chromosome 5 (61). The haplotype distribution among other genes localized to mouse Chromosome 5 is shown in Figure 5. The best gene order (53) \pm SD (52) indicated the gene order: centromere *Qdpr*-0.9 cM \pm 0.9 cM-*Sod3*-7.0 cM \pm 2.4 cM-*Cncg*.

Lung Alveolar Epithelial Type II Cells Predominantly Express EC-SOD

We used the technique of *in situ* hybridization to determine the cell type(s) expressing EC-SOD in the mouse lung. Normal mouse lungs were inflation-fixed, cut into 5- μ m sections, and hybridized overnight to digoxigenin-labeled sense and antisense strand EC-SOD cRNA. Labeling with an antisense-strand cRNA probe revealed a uniform pattern of distribution across each of the animals studied. Figure 6A demonstrates a typical pattern of observed labeling. Throughout this section, a purple-blue stain can be seen, predominantly over alveolar epithelial cells, in a pattern that is entirely consistent with that of alveolar Type II cells. Alveolar macrophages, a cell type occasionally seen in normal mouse lung sections, were also found to stain positively (not illustrated). Under the conditions of our *in situ* detection system, we were unable to detect labeling over endothelial cells, bronchial epithelial cells, bronchiolar epithelial cells, fibroblasts, smooth-muscle cells, or pleural mesothelial cells. When the tissue sections were incubated with a digoxigenin-labelled sense-strand, no signal was appreciable (Figure 6B).

Discussion

We have now cloned and characterized a full-length mouse EC-SOD cDNA. Of three EC-SODs now characterized, the mouse EC-SOD cDNA is the largest (1,834 bp), fol-

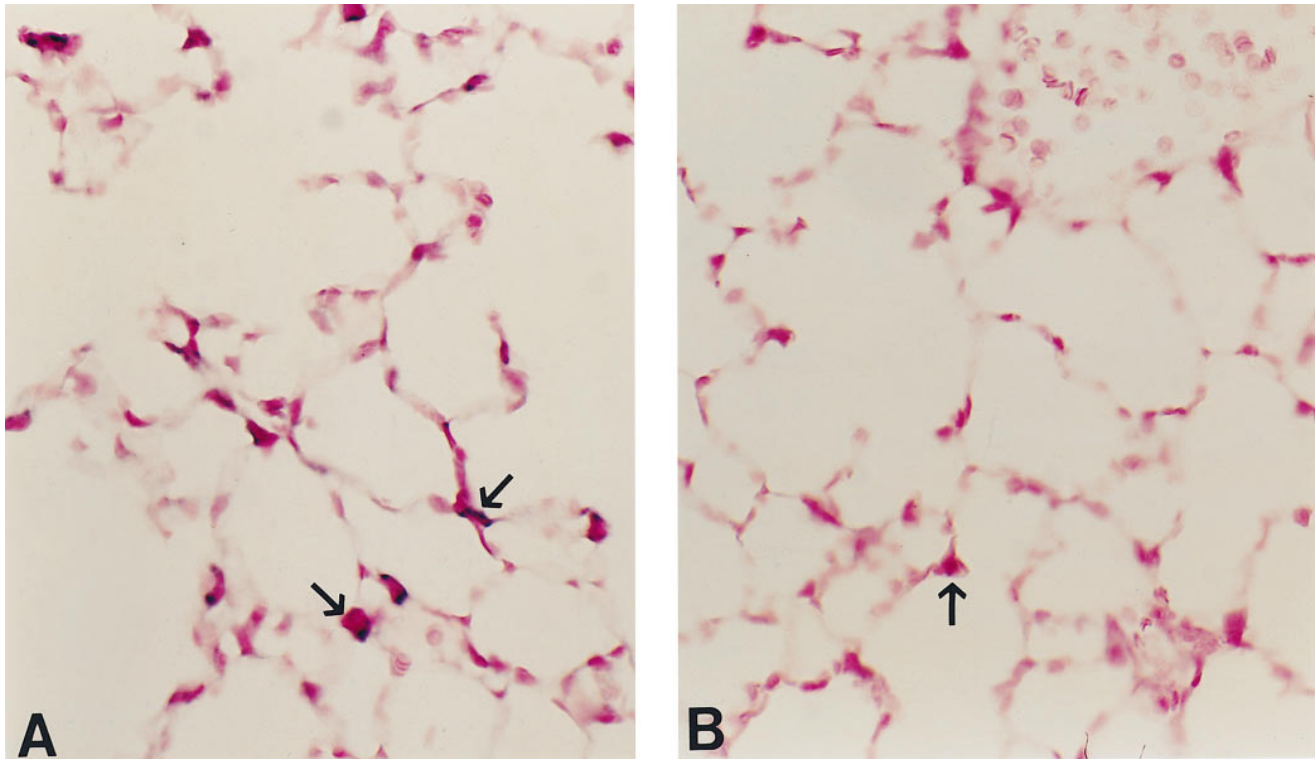


Figure 6. Expression of EC-SOD mRNA in normal mouse lung shown by *in situ* hybridization. (A) Purple-blue alkaline phosphatase staining, which is easily detectable in alveolar epithelial Type II cells (arrow). The purple-blue staining is distinct from the reddish-pink background staining. (B) Sense strand negative control, demonstrating essentially undetectable background purple-blue precipitate. The tissue sections were photographed at $\times 100$ magnification. Although not shown in this figure, purple-blue staining was seen in alveolar macrophages. We were unable to detect a signal in bronchial epithelial, bronchial, or vascular smooth muscle, fibroblasts, or endothelial cells.

lowed by rat (1,729 bp) (28) and human (1,432 bp) EC-SOD cDNA (27, 32). As might be expected, computer-based homology search routines performed according to the BLAST algorithm (45) and using nonredundant protein and nucleic acid databases demonstrate highly significant matches of mouse EC-SOD to rat and human EC-SOD, followed by less significant matches to CuZn-SOD sequences (data not shown). Of note is that Mn-SOD does not show any homology, at either the protein or nucleic acid level, to EC-SOD. Amino-acid sequence comparisons show that the mouse and rat EC-SODs are more similar to each other (79%) than to human EC-SOD (60%). The magnitude of the species-specific differences in similarity for EC-SOD is less than that seen with either CuZn-SOD or Mn-SOD. For example, mouse and rat CuZn-SOD show 97% similarity (62), mouse and human CuZn-SOD show 84% similarity (62), and rat and human CuZn-SOD show 83% similarity (63). Mn-SOD is highly conserved between species, with 96% sequence similarity between mouse and rat, 94% similarity between mouse and human, and 93% similarity between rat and human Mn-SOD (64–66).

The evolutionary pressures that have allowed more interspecies flexibility in the structure of SOD3 are unclear. The EC-SOD primary structure can be separated into four segments. Segment 1 includes the signal peptide. Segment 2 encompasses the mature, glycosylated NH₂-terminus,

where the majority of sequence diversity occurs. Segment 3 shows high sequence conservation with SOD1, and in particular with residues critical to enzyme catalysis and function. Segment 4 contains the COOH-terminal charged basic region important in heparan binding. One explanation for the lack of sequence conservation in segment 2 could be that the role of Segment 2 in the biology of EC-SOD is less pivotal than that of the other segments of this protein. Another possibility is that the gene for human EC-SOD is not the true gene homologue of mouse or rat EC-SOD. However, we find this unlikely, since human (31) and mouse (unpublished data) genomic Southern blots probed at low stringencies demonstrate a unique banding pattern consistent with a single gene locus for EC-SOD. Consistent with the variation seen in amino-acid sequence between species is the finding that polyclonal antibodies generated against human EC-SOD do not cross-react with mouse or rat EC-SOD (unpublished data).

Translation of the mouse cDNA predicts a 251-amino-acid secretory protein of 27,400 D, which is in excellent agreement with *in vitro*-translated protein from the mouse EC-SOD cRNA (data not shown). NH₂-terminal sequence analysis of purified mature EC-SOD demonstrates the initial residues to be Ser-Ser-Phe-. These results would indicate that mouse EC-SOD, when initially synthesized, contains a 24-amino-acid precursor peptide. However, we

propose that this precursor peptide contains both a signal peptide and a propeptide. Computer algorithms that predict the site of cotranslational signal-peptide cleavage suggest that signal-peptide cleavage is most likely to occur between residues 18 and 19, or 20 and 21, and that cleavage between residues 24 and 25 is highly unlikely (47, 54). In general, most signal-peptide cleavage sites follow the “-3, -1” rule, which states that amino acids found at positions -3 and -1 contain small aliphatic side chains (e.g., Ala, Ser, Gly for position -1, and Ala, Cys, Ser, Thr for position -3) (67, 68). If the amino-acid residues at these positions contain large and/or bulky side chains, are sterically constrained (e.g., Pro), or are charged, then signal-peptide cleavage can be either prevented or redirected to other position(s) within the precursor protein (54). Signal peptide cleavage between residues 24 and 25 is therefore highly unlikely, because the amino acid residues that correspond to positions -3 and -1 would be Pro and Glu, two amino acids that appear to preclude cleavage. What could be the role of this putative propeptide? One possibility is that the propeptide acts as an adapter to allow or facilitate signal peptide function, signal peptide cleavage, or post-translational modification or transport. Such a function could be necessary if the seven-amino-acid insertion sequence at positions 3 through 9 in mature mouse EC-SOD would otherwise interfere with these possible functions. For example, propeptides can affect the specific site of cotranslational signal peptide cleavage (46), as well as modify the efficiency of cotranslational translocation (69).

Tissue-specific gene expression studies show the kidney and lung to be the major sources of EC-SOD mRNA in the mouse. When the same tissues were measured for EC-SOD enzyme activity, the lung showed 10 times the level seen in all other tissues, with the kidneys containing the second highest level (19). Tissues that had low mRNA levels, such as skeletal muscle, also had minimally detectable EC-SOD enzyme activity. Thus, tissue enzyme levels appear to correlate well with mRNA levels for EC-SOD. These results suggest that EC-SOD remains localized to tissues that express and secrete EC-SOD. However, another possibility is that factors important in tissue localization of EC-SOD (e.g., heparan sulfates in the interstitial matrix, and/or proteolytic enzymes) are coregulated along with EC-SOD. We favor the former explanation, because transgenic mice that overexpress human EC-SOD under the direction of the highly lung-specific surfactant protein C promoter show transgenic human EC-SOD protein to be entirely contained within the lung and not detectable in other tissues (unpublished data).

Because EC-SOD is found at such high levels in the mouse lung, and shows high levels of gene expression, we sought to identify the cell type(s) that express EC-SOD in mouse lung. To our knowledge, the only previous studies that address the question of which cell types express EC-SOD have been done exclusively with various cell lines grown in cell culture. These results show that 25 different fibroblast cell lines and two glial cell lines express EC-SOD, whereas no expression is seen in six endothelial or two epithelial cell lines (34). Using the technique of *in situ* hybridization, we found that the predominant source of EC-SOD mRNA was localized to alveolar epithelial cells

whose pattern of staining is entirely consistent with alveolar Type II cells. Smaller amounts of positively staining signal were also present in alveolar macrophages. Under the conditions used, we could not detect expression of EC-SOD mRNA in alveolar Type I epithelium, bronchial epithelium, vascular endothelium, or interstitial fibroblasts. This pattern of gene expression in the lung is similar to that seen with inducible nitric oxide synthetase (iNOS) in both the rat (70, 71) and human (70). In these examples, iNOS has been shown to be predominantly expressed by alveolar macrophages and alveolar epithelial Type II cells, with the subsequent release of nitric oxide (NO). It has been shown that the superoxide anion species reacts with NO to produce the toxic peroxynitrite anion species at diffusion-limited rates (72). We speculate that one role of EC-SOD may be to maintain low levels of superoxide species in the alveolar region. Thus, *in vivo* conditions that upregulate iNOS expression with resultant increases in NO in the lung would be predicted to benefit from low levels of superoxide species. Such conditions would include a wide variety of inflammatory lung disorders, such as inhalation of pulmonary irritants (73) and intratracheal instillation of lipopolysaccharide (LPS) (71).

The physical mapping of a gene locus can lead to serendipitous linkages to models of genetic disease and further biologic insights. In the current study, the mouse *Sod3* gene was mapped to a position in the middle of mouse Chromosome 5. The *Sod3* gene was tightly linked to the *Qdpr* gene, suggesting that the human EC-SOD homologue will map close to the same location (4p15.3) as the human *QDPR* locus. In accord with this prediction, the human gene *SOD3* has recently been mapped to the short arm of human Chromosome 4 through somatic cell hybrid analysis (32). A comprehensive list of all genetic loci reported to map to mouse Chromosome 5 has been compiled (61). On the basis of this compilation, it can be discerned that *Sod3* maps to a region on Chromosome 5 that is consistent with the genetic mapping of *gad*, a recently described animal model of central distal axonopathy in primary sensory neurons (74–76). This finding is very exciting because mutations in *SOD1* have been linked to familial amyotrophic lateral sclerosis (Lou Gehrig's disease) (6, 77). Experiments are underway that will directly examine the possibly critical role of alterations in *Sod3* in the pathogenesis of these types of disorders.

In conclusion, mouse EC-SOD is encoded within an 1,834-bp mRNA whose open-reading-frame analysis predicts a 251-amino-acid precursor protein. NH₂-terminal sequence analysis of purified mature mouse EC-SOD protein, along with computer-assisted predictions of the site of signal-peptidase cleavage, suggest that when initially synthesized, this protein contains a 24-amino-acid prepropeptide followed by a 227-amino-acid mature protein domain. The role of the putative propeptide in co- and/or posttranslational protein processing has not yet been determined. Amino acid homology comparisons of mouse, rat, and human EC-SOD demonstrate more flexibility in allowing for mutations in its primary sequence, as compared with much greater conservation within the CuZn-SODs and Mn-SODs. Of nine mouse tissues examined, the kidney and lung contained the highest levels of EC-

SOD mRNA. Expression of EC-SOD in the lung occurred predominantly in alveolar Type II epithelial cells and alveolar macrophages, suggesting that these cell types play a central role in regulating extracellular antioxidant function.

Acknowledgments: Rodney J. Folz is a Parker B. Francis Fellow in Pulmonary Research. The authors would like to thank Ken Kuzenski and Dr. Emily K. Folz for editing this manuscript. This work was funded in part by National Institutes of Health Grants GH 00734 (to M.F.S.), HL 49542 (to J.J.E.), HL31992 (to J.D.C.), and HL55166 (to R.J.F.), and by a Duke University Medical Center Small Research Grant (to R.J.F.).

References

- McCord, J. M., and I. Fridovich. 1969. Superoxide dismutase: an enzymic function for erythrocyte hemocuprein. *J. Biol. Chem.* 244:6049-6055.
- Chang, L.-Y., J. W. Slot, H. J. Geuze, and J. D. Crapo. 1988. Molecular immunocytochemistry of the CuZn superoxide dismutase in rat hepatocytes. *J. Cell Biol.* 107:2169-2179.
- Keller, G.-A., T. G. Warner, K. S. Steimer, and R. A. Hallelwell. 1991. CuZn superoxide dismutase is a peroxisomal enzyme in human fibroblasts and hepatoma cells. *Proc. Natl. Acad. Sci. USA* 88:7381-7385.
- Crapo, J. D., T. Oury, C. Rabouille, J. W. Slot, and L.-Y. Chang. 1992. Copper, zinc superoxide dismutase is primarily a cytosolic protein in human cells. *Proc. Natl. Acad. Sci. USA* 89:10405-10409.
- Tan, Y. H., J. Tischfield, and F. H. Ruddle. 1973. The linkage of genes for the human interferon-induced antiviral protein and indophenol oxidase-B traits to chromosome G-21. *J. Exp. Med.* 137:317-330.
- Rosen, D. R., T. Siddique, D. Patterson, D. A. Figlewicz, P. Sapp, A. Hentati, D. Donaldson, J. Goto, J. P. O'Regan, H.-X. Deng, Z. Rahmani, A. Krizus, D. McKenna-Yasek, A. Cayabyab, S. M. Gaston, R. Berger, R. E. Tanzi, J. J. Halperin, B. Herzfeldt, R. Van den Bergh, W.-Y. Hung, T. Bird, G. Deng, D. W. Mulder, C. Smyth, N. G. Laing, E. Soriano, M. A. Pericak-Vance, J. Haines, G. A. Rouleau, J. S. Gusella, H. R. Horvitz, and R. H. Brown, Jr. 1993. Mutations in Cu/Zn superoxide dismutase gene are associated with familial amyotrophic lateral sclerosis. *Nature* 362:59-62.
- Gurney, M. E., H. Pu, A. Y. Chiu, M. C. D. Canto, C. Y. Polchow, D. D. Alexander, J. Caliendo, A. Hentati, Y. W. Kwon, H.-X. Deng, W. Chen, P. Zhai, R. L. Sufit, and T. Siddique. 1994. Motor neuron degeneration in mice that express a human Cu,Zn superoxide dismutase mutation. *Science* 264:1772-1775.
- Creagan, R., J. Tischfield, F. Ricciuti, and F. H. Ruddle. 1973. Chromosome assignments of genes in man using mouse-human somatic cell hybrids: mitochondrial superoxide dismutase (indophenol oxidase-B, tetrameric) to chromosome 6. *Humangenetik* 20:203-209.
- Weisiger, R. A., and I. Fridovich. 1973. Mitochondrial superoxide dismutase: site of synthesis and intramitochondrial localization. *J. Biol. Chem.* 248:4793-4796.
- Folz, R. J., and J. D. Crapo. 1994. Pulmonary oxygen toxicity. In *Current Pulmonology*, 15th ed. D. F. Tierney, editor. Mosby Year-Book, Chicago. 113-136.
- St. Clair, D. K., T. D. Oberley, K. E. Muse, and W. H. St. Clair. 1993. Expression of manganese superoxide dismutase promotes cellular differentiation. *Free Radic. Biol. Med.* 16:275-282.
- Wispe, J. R., B. B. Warner, J. C. Clark, C. R. Day, J. Neuman, S. W. Glasser, J. D. Crapo, L.-Y. Chang, and J. A. Whitsett. 1992. Human Mn-superoxide dismutase in pulmonary epithelial cells of transgenic mice confers protection from oxygen injury. *J. Biol. Chem.* 267:23937-23941.
- Wong, G. H. W., and D. V. Goeddel. 1988. Induction of manganese superoxide dismutase by tumor necrosis factor: possible protective mechanism. *Science* 242:941-944.
- Wong, G. H. W., J. H. Elwell, L. W. Oberley, and D. V. Goeddel. 1989. Manganese superoxide dismutase is essential for cellular resistance to cytotoxicity of tumor necrosis factor. *Cell* 58:923-931.
- Marklund, S. L., E. Holme, and L. Hellner. 1982. Superoxide dismutase in extracellular fluids. *Clin. Chim. Acta* 126:41-51.
- Marklund, S. L., A. Bjelle, and L. G. Elmqvist. 1986. Superoxide dismutase isoenzymes of the synovial fluid in rheumatoid arthritis and in reactive arthritides. *Ann. Rheum. Dis.* 45:847-851.
- Sandstrom, J., K. Karlsson, T. Edlund, and S. L. Marklund. 1993. Heparin-affinity patterns and composition of extracellular superoxide dismutase in human plasma and tissues. *Biochem. J.* 294:853-857.
- Oury, T. D., B. J. Day, and J. D. Crapo. 1996. Extracellular superoxide dismutase in vessels and airways of humans and baboons. *Free Radic. Biol. Med.* 20:957-965.
- Marklund, S. L. 1984. Extracellular superoxide dismutase and other superoxide dismutase isoenzymes in tissues from nine mammalian species. *Biochem. J.* 222:649-655.
- Marklund, S. L. 1982. Human copper-containing superoxide dismutase of high molecular weight. *Proc. Natl. Acad. Sci. USA* 79:7634-7638.
- Stromqvist, M., J. Holgersson, and B. Samuelsson. 1991. Glycosylation of extracellular superoxide dismutase studied by high-performance liquid chromatography and mass spectrometry. *J. Chromatogr.* 548:293-301.
- Adachi, T., T. Koda, H. Ohta, K. Hayashi, and K. Hirano. 1992. The heparin binding site of human extracellular-superoxide dismutase. *Arch. Biochem. Biophys.* 297:155-161.
- Sandstrom, J., L. Carlsson, S. L. Marklund, and T. Edlund. 1992. The heparin-binding domain of extracellular superoxide dismutase C and formation of variants with reduced heparin affinity. *J. Biol. Chem.* 267:18205-18209.
- Karlsson, K., and S. L. Marklund. 1988. Extracellular superoxide dismutase in the vascular system of mammals. *Biochem. J.* 255:223-228.
- Adachi, T., H. Ohta, H. Yamada, A. Futenma, K. Kato, and K. Hirano. 1992. Quantitative analysis of extracellular-superoxide dismutase in serum and urine by ELISA with monoclonal antibody. *Clin. Chim. Acta* 212:89-102.
- Karlsson, K., A. Edlund, J. Sandstrom, and S. L. Marklund. 1993. Proteolytic modification of the heparin-binding affinity of extracellular superoxide dismutase. *Biochem. J.* 290:623-626.
- Hjalmarsson, K., S. L. Marklund, A. Engstrom, and T. Edlund. 1987. Isolation and sequence of complementary DNA encoding human extracellular superoxide dismutase. *Proc. Natl. Acad. Sci. USA* 84:6340-6344.
- Willems, J., A. Zwijsen, H. Slegers, S. Nicolai, J. Bettadapura, J. Raymackers, and T. Scarcez. 1993. Purification and sequence of rat extracellular superoxide dismutase B secreted by C₆ glioma. *J. Biol. Chem.* 268:24614-24621.
- Perry, A. C. F., R. Jones, and L. Hall. 1993. Isolation and characterization of a rat cDNA clone encoding a secreted superoxide dismutase reveals the epididymis to be a major site of its expression. *Biochem. J.* 293:21-25.
- Carlsson, L. M., S. L. Marklund, and T. Edlund. 1996. The rat extracellular superoxide dismutase dimer is converted to a tetramer by the exchange of a single amino acid. *Proc. Natl. Acad. Sci. USA* 93:5219-5222.
- Folz, R. J., and J. D. Crapo. 1994. Extracellular superoxide dismutase (SOD3): tissue-specific expression, genomic characterization, and computer-assisted sequence analysis of the human EC-SOD gene. *Genomics* 22:162-171.
- Hendrickson, D. J., J. H. Fisher, C. Jones, and Y.-S. Ho. 1990. Regional localization of human extracellular superoxide dismutase gene to 4pter-q21. *Genomics* 8:736-738.
- Marklund, S. L. 1984. Extracellular superoxide dismutase in human tissues and human cell lines. *J. Clin. Invest.* 74:1398-1403.
- Marklund, S. L. 1990. Expression of extracellular superoxide dismutase by human cell lines. *Biochem. J.* 266:213-219.
- Marklund, S. L. 1992. Regulation by cytokines of extracellular superoxide dismutase and other superoxide dismutase isoenzymes in fibroblasts. *J. Biol. Chem.* 267:6696-6701.
- Stralin, P., and S. L. Marklund. 1994. Effects of oxidative stress on expression of extracellular superoxide dismutase, CuZn-superoxide dismutase and Mn-superoxide dismutase in human dermal fibroblasts. *Biochem. J.* 298:347-352.
- Carlsson, L. M., J. Jonsson, T. Edlund, and S. L. Marklund. 1995. Mice lacking extracellular superoxide dismutase are more sensitive to hyperoxia. *Proc. Natl. Acad. Sci. USA* 92:6264-6268.
- Freeman, B. A., and J. D. Crapo. 1981. Hyperoxia increases oxygen radical production in rat lungs and lung mitochondria. *J. Biol. Chem.* 256:10986-10992.
- Chomczynski, P., and N. Sacchi. 1987. Single-step method of RNA isolation by acid guanidinium thiocyanate-phenol-chloroform extraction. *Anal. Biochem.* 162:156-159.
- Sanger, F., S. Nicklen, and A. R. Coulson. 1977. DNA sequencing with chain-terminating inhibitors. *Proc. Natl. Acad. Sci. USA* 74:5463-5467.
- Oury, T. D., J. D. Crapo, Z. Valnickova, and J. J. Enghild. 1996. Human extracellular superoxide dismutase is a tetramer composed of two disulfide-linked dimers: a simplified, high yield purification of extracellular superoxide dismutase. *Biochem. J.* 317:51-57.
- Crapo, J. D., J. M. McCord, and I. Fridovich. 1978. Preparation and assay of superoxide dismutases. *Methods Enzymol.* 53:382-390.
- Matsudaira, P. 1987. Sequence from picomole quantities of proteins electroblotted onto polyvinylidene difluoride membranes. *J. Biol. Chem.* 262:10035-10038.
- Enghild, J. J., G. Salvesen, S. A. Hefta, I. B. Thogersen, S. Rutherford, and S. V. Pizzo. 1991. Chondroitin 4-sulfate covalently cross-links the chains of the human blood protein pre-alpha-inhibitor. *J. Biol. Chem.* 266:747-751.
- Altschul, S. F., W. Gish, W. Miller, E. W. Myers, and D. J. Lipman. 1990. Basic local alignment search tool. *J. Mol. Biol.* 215:403-410.
- Folz, R. J., and J. I. Gordon. 1986. Deletion of the propeptide from human preproalipoprotein A-II redirects co-translational processing by signal peptidase. *J. Biol. Chem.* 261:14752-14759.
- Folz, R. J., and J. I. Gordon. 1987. Computer-assisted predictions of signal peptidase processing sites. *Biochem. Biophys. Res. Commun.* 146:870-877.
- Nei, M. 1987. *Molecular Evolutionary Genetics*. Columbia University Press, New York. 293-298.
- Seldin, M. F., H. C. Morse, J. P. Reeves, C. L. Scribner, R. C. LeBoeuf, and A. D. Steinberg. 1988. Genetic analysis of autoimmune *gld* mice I. Identifi-

- cation of a restriction fragment length polymorphism closely linked to the *gld* mutation within a conserved linkage group. *J. Exp. Med.* 167:688–693.
50. Maniatis, T., E. F. Fritsch, and J. Sambrook. 1982. *Molecular Cloning: A Laboratory Manual*. Cold Spring Harbor Laboratory, New York.
 51. Pittler, S. J., A. K. Lee, M. R. Altherr, T. A. Howard, M. F. Seldin, R. L. Hurwitz, J. J. Wasmuth, and W. Baehr. 1992. Primary structure and chromosomal localization of human and mouse rod photoreceptor cGMP-gated channel. *J. Biol. Chem.* 267:6257–6262.
 52. Green, E. L. 1981. Linkage, recombination and mapping. In *Genetics and Probability in Animal Breeding Experiments*. E. L. Green, editor. Macmillan, New York. 77–113.
 53. Bishop, D. T. 1985. The information content of phase-known matings for ordering genetic loci. *Genet. Epidemiol.* 2:349–361.
 54. Folz, R. J., S. F. Nothwehr, and J. I. Gordon. 1988. Substrate specificity of eukaryotic signal peptidase. *J. Biol. Chem.* 263:2070–2078.
 55. Von Heijne, G. 1987. *Sequence Analysis in Molecular Biology*. Academic Press, San Diego, CA.
 56. Sandstrom, J., K. Karlsson, A. Edlund, and S. L. Marklund. 1993. Proteolytic modification of heparin-binding affinity of extracellular superoxide dismutase. *Biochem. J.* 290:623–626.
 57. Oury, T. D., L.-Y. Chang, S. L. Marklund, B. J. Day, and J. D. Crapo. 1994. Immunocytochemical localization of extracellular superoxide dismutase in human lung. *Lab. Invest.* 70:889–898.
 58. Tainer, J. A., E. D. Getzoff, K. M. Beem, J. S. Richardson, and D. C. Richardson. 1982. Determination and analysis of the 2 Å structure of copper, zinc superoxide dismutase. *J. Mol. Biol.* 160:181–217.
 59. Saunders, A. M., and M. F. Seldin. 1990. A molecular genetic linkage map of mouse chromosome 7. *Genomics* 8:525–535.
 60. Watson, M. L., P. D'Eustachio, B. A. Mock, A. D. Steinberg, C. Herbert, I. Morse, R. J. Oakley, T. A. Howard, J. M. Rochelle, and M. F. Seldin. 1992. A linkage map of mouse chromosome 1 using an interspecific cross segregating for the *gld* autoimmunity mutation. *Mammalian Genome* 2:158–171.
 61. Kozak, C. A., and D. A. Stephenson. 1993. Mouse chromosome 5. *Mammalian Genome* 4:S72–S87.
 62. Bewley, G. C. 1988. cDNA and deduced amino acid sequence of murine Cu-Zn superoxide dismutase. *Nucleic Acids Res.* 16:2728.
 63. Ho, Y.-S., and J. D. Crapo. 1987. cDNA and deduced amino acid sequences of rat copper-zinc containing superoxide dismutase. *Nucleic Acids Res.* 15:6746.
 64. Hallewell, R. A., G. T. Mullenbach, M. M. Stempien, and G. I. Bell. 1986. Sequence of a cDNA coding for mouse manganese superoxide dismutase. *Nucleic Acids Res.* 14:9539.
 65. Ho, Y.-S., and J. D. Crapo. 1987. Nucleotide sequences of cDNAs coding for rat manganese-containing superoxide dismutase. *Nucleic Acids Res.* 15:10070.
 66. Ho, Y.-S., and J. D. Crapo. 1988. Isolation and characterization of complementary DNAs encoding human manganese-containing superoxide dismutase. *FEBS Lett.* 229:256–260.
 67. Von Heijne, G. 1983. Patterns of amino acids near signal-sequence cleavage sites. *Eur. J. Biochem.* 133:17–21.
 68. Von Heijne, G. 1986. A new method for predicting signal sequence cleavage sites. *Nucleic Acids Res.* 14:4683–4690.
 69. Folz, R. J., and J. I. Gordon. 1987. The effects of deleting the propeptide from human preproapolipoprotein A-I on Co-translational translocation and signal peptidase processing. *J. Biol. Chem.* 262:17221–17230.
 70. Kobzik, D. S., D. S. Bredt, C. J. Lowenstein, J. Drazin, B. Gaston, D. Sugarbaker, and J. S. Stamler. 1993. Nitric oxide synthase in human and rat lung: immunocytochemical and histochemical localization. *Am. J. Respir. Cell Mol. Biol.* 9:371–377.
 71. Warner, R. L., R. Paine, III, P. J. Christensen, M. A. Marletta, M. K. Richards, S. E. Wilcoxon, and P. A. Ward. 1995. Lung sources and cytokine requirements for *in vivo* expression of inducible nitric oxide synthase. *Am. J. Respir. Cell Mol. Biol.* 12:649–661.
 72. Huie, R. E., and S. Padmaja. 1993. The reaction of NO with superoxide. *Free Radic. Res. Commun.* 18:195–199.
 73. Punjabi, C. J., J. D. Laskin, K. J. Pendino, N. L. Goller, S. K. Durham, and D. L. Laskin. 1994. Production of nitric oxide by rat type II pneumocytes: increased expression of inducible nitric oxide synthase following inhalation of a pulmonary irritant. *Am. J. Respir. Cell Mol. Biol.* 11:165–172.
 74. Yamazaki, K., A. Sakakibara, T. Tomita, M. Mukoyama, and T. Kikuchi. 1987. Location of gracile axonal dystrophy (*gad*) on chromosome 5 of the mouse. *Jpn. J. Genet.* 62:479–484.
 75. Mukoyama, M., K. Yamazaki, T. Kikuchi, and T. Tomita. 1989. Neuropathology of gracile axonal dystrophy (GAD) mouse. *Acta Neuropathol.* 79:294–299.
 76. Kikuchi, T., M. Mukoyama, K. Yamazaki, and H. Moriya. 1990. Axonal degeneration of ascending sensory neurons in gracile axonal dystrophy mutant mouse. *Acta Neuropathol.* 80:145–151.
 77. McNamara, J. O., and I. Fridovich. 1993. Did radicals strike Lou Gehrig? *Nature* 362:20–21.